

terms indeed to yield Eqs. (10), (14), (16), (17), (18), (19), and (20) which probably go as far as one would like to take the expansion.

This approach has also demonstrated the correspondence between the order of the spherical harmonic or the tensor expansion and the order of tensor transport quantities. Usually these quantities are in terms of the particular or peculiar velocity, the velocity referred to an average velocity frame of reference ($\mathbf{v}-\langle\mathbf{v}\rangle$ rather than \mathbf{v}). Since this frame of reference changes with time and place it is not suited to the spherical harmonic expansion unless the average velocity has at least a large constant part. Usually the peculiar velocity terms will have to be calculated from the rest frame velocity expansion, clumsy though it may seem.

The assumption of a scalar pressure requires only the zero and first order spherical harmonic terms, while an anisotropic pressure will necessitate second order terms and a pressure transport tensor must imply third order terms.

Even if this clarification of the spherical harmonic expansion does not produce a rewarding attack on plasma problems it should lead to a clearer understanding of basic expansions of the distribution function and the relation of this approach to others.

ACKNOWLEDGMENTS

It is a pleasure to acknowledge suggestions and criticism from Dr. I. P. Shkarofsky and Dr. M. P. Bachynski.

Nuclear Spin Relaxation in Liquid Helium 3†

F. J. LOW* AND H. E. RORSCHACH
The Rice University, Houston, Texas
(Received July 11, 1960)

The longitudinal relaxation time of liquid He³ has been measured as a function of temperature above 1°K and of magnetic field below 13 kgauss in a number of sample containers. At a temperature of 2.0°K and in a magnetic field of 10 kgauss the longitudinal relaxation time, T_1 , varied with the sample container from 60 seconds to 400 seconds. The transverse relaxation time, T_2 , was measured by a new method and was approximately 30 seconds at a field of 10 kgauss in all sample containers. T_1 was determined as a function of magnetic field at 2.0°K in a single sample container; the values increased from less than 50 seconds in approximately zero field to 400 seconds at 13 kgauss. An impurity relaxation model is proposed to explain the T_1 results. By assuming both wall relaxation and a bulk relaxation given by the Bloembergen, Purcell, and Pound theory, the dependence of T_1 on pressure and temperature can be quantitatively understood. The low values of T_2 are inconsistent with the Bloembergen, Purcell, and Pound theory and may be due to the presence of paramagnetic impurities in suspension in the bulk liquid.

INTRODUCTION

USING adiabatic fast passage techniques, we have measured the longitudinal and transverse nuclear magnetic relaxation times, T_1 and T_2 , in liquid He³ contained in sample chambers of different sizes and materials. The T_1 measurements supplement recently reported values obtained at three different laboratories.¹⁻³ Our values of T_1 versus magnetic field do not agree with some recent measurements of Romer² which gave a T_1 independent of field. The T_2 measurements, the first reported for liquid He³, were obtained by a new method which makes possible the measurement of long transverse relaxation times. The measured values of T_2 are an order of magnitude less than T_1 .

Nuclear relaxation in liquid He³ has been analyzed

by various workers¹⁻⁴ in terms of the Bloembergen, Purcell, and Pound theory for classical liquids.⁵ It would be surprising if the intrinsic relaxation in liquid He³ were completely described by this theory since it does not take account of any quantum statistical effects. Nevertheless, we can show that most of the data above 1°K are compatible with this theory if impurity effects are considered. To explain the various T_1 and T_2 results we propose an impurity relaxation model based on a wall relaxation in parallel with the bulk relaxation. A reason for the inequality of T_1 and T_2 will be suggested.

The experimental technique will be described in detail and the method of measuring T_2 will be discussed. During the course of these measurements nuclear maser effects were observed.

† Supported by a grant from the Robert A. Welch Foundation.

* Now at Texas Instruments Inc., Dallas, Texas.

¹ G. Careri, I. Modena, and M. Santini, *Nuovo cimento* **13**, 207 (1959), and private communication.

² R. H. Romer, *Phys. Rev.* **115**, 1415 (1959); *Phys. Rev.* **117**, 1183 (1960).

³ R. L. Garwin and H. A. Reich, *Phys. Rev.* **115**, 1478 (1959).

⁴ W. M. Fairbank and G. K. Walters, *Symposium on Liquid, and Solid Helium 3* (Ohio State University Press, Columbus, Ohio, 1957).

⁵ N. Bloembergen, E. M. Purcell, and R. V. Pound. *Phys. Rev.* **73**, 679 (1948).

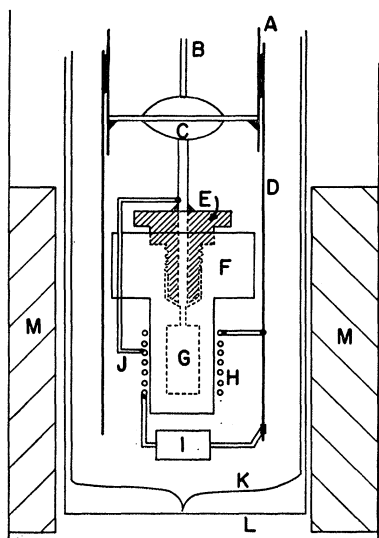


FIG. 1. Schematic of cryogenic apparatus. A-outer wall of transmission line; B-He³ capillary and inner conductor of transmission line; C-kovar seal; D-brass shield; E-brass plug which forms seal to nylon; F-nylon sample chamber; G-cylindrical He³ space; H-rf solenoid; I-tuning capacitor; J-coil tap; K-glass helium Dewar; L-brass nitrogen Dewar; M-12-in. Varian magnet with 1 1/4 in. gap.

EXPERIMENTAL DETAILS

The measurements were carried out on He³ with less than 1% He⁴ contained in various nylon sample chambers. At the beginning of each run, the gas-handling apparatus and sample chamber were evacuated to a pressure of approximately 10^{-6} mm Hg. The He³ was passed through a liquid He⁴ trap and admitted to the sample chamber through a 0.011 inch i.d. stainless steel capillary. At the conclusion of each run the sample was returned to its storage flask by means of a glass Toepler pump. This pump was a mercury-in-glass manometer which could also be used to measure the pressure in the system. The nylon sample chambers employ a unique metal-dielectric seal shown schematically in Fig. 1. The brass plug screws into the top of the nylon sample chamber. The plug is tapered at the bottom to form a tight fit with an identical taper in the nylon. The differential thermal contraction gives a low-temperature seal that is tight to superfluid helium. The sample chambers can be opened and resealed. The length of the cylindrical He³ space was 12 mm while the diameter was 3, 5, and 8 mm in the various chambers. On two runs, the walls of the He³ space were lined with Pyrex, and on another run they were lined with waxed paper.

A glass helium Dewar and a metal nitrogen Dewar were used to obtain a one inch working space in the 1 1/4 inch magnet gap. The lowest temperature obtained with a KS 200 Consolidated Electrodynamics diffusion pump was 0.92°K.

Figure 1 shows the sample chamber and tuned circuit at the bottom of the transmission line. The outer

conductor of the transmission line was thin wall monel tubing. Copper-plated stainless steel capillary 1/32 inch in diameter served both as the inner conductor and as the filling tube leading to the sample chamber. To reduce microphonics, the center conductor was held rigidly in place by means of Kovar seals. The signal-noise ratio was also improved by excluding the liquid helium from the interior of the transmission line. The silver mica tank circuit capacitor changed by less than 4% when cooled from room temperature to 4°K and was constant over the liquid helium range. The rf solenoid was wound with No. 26 enameled copper wire and cemented in place around the sample chamber. The Q of a typical tank circuit was 400 at low temperatures and was constant to within a percent over the helium range. The Q at room temperature was of the order of 100.

The nuclear resonance signals observed in this experiment were detected by a balanced detector patterned after that of Thomas and Huntoon⁶ (see Fig. 2). This detector is sensitive to impedance changes at the top of the transmission line. The transmission line transforms the impedance of the tank circuit, Z_L , to an impedance Z_T at the top of the line. If Z_T is purely resistive, then the detector will be sensitive only to resistive changes. If Z_T is a complex impedance, then the detector will be sensitive both to resistive and reactive changes. The impedance observed at the top of the line will depend on the impedance of the tank circuit, Z_L , and the properties of the transmission line. If line losses are neglected, the impedance observed at the top of a transmission line of length L is:⁷

$$Z_T = Z_0 \frac{Z_L \cos(2\pi L/\lambda) + jZ_0 \sin(2\pi L/\lambda)}{Z_0 \cos(2\pi L/\lambda) + jZ_L \sin(2\pi L/\lambda)},$$

where Z_0 is the characteristic impedance of the line. If $L = \lambda/8$, then the impedance at the top is

$$Z_T = Z_0 \frac{Z_L + jZ_0}{Z_0 + jZ_L}.$$

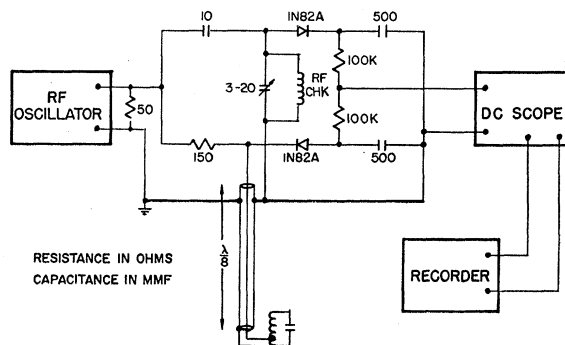


FIG. 2. Schematic of detector circuit.

⁶ H. A. Thomas and R. D. Huntoon, Rev. Sci. Instr. 20, 516 (1949).

⁷ American Institute of Physics Handbook (McGraw-Hill Book Company, Inc., New York, 1957), pp. 5-50.

If the tank circuit is tapped to match the characteristic impedance of the line ($Z_L = Z_0$), then $Z_T = Z_0$. When the tank circuit impedance changes by dZ_L , then the impedance at the top changes by

$$dZ_T = \frac{Z_0}{Z_0 + jZ_L} (1 - j) dZ_L = -j dZ_L.$$

Thus, when the line is terminated with its characteristic impedance, the impedance observed at the top of the line is real, regardless of length, but as a result of the $\frac{1}{8}$ wave line an incremental change in the impedance at the bottom is observed at the top as an equal but orthogonal change. Under these conditions, the detector will be sensitive to dispersion in the tank circuit, but not to absorption. If the line is one-quarter wave long, the impedance at the top is still Z_0 , but $dZ_T = -dZ_L$. The detector will now be sensitive to absorption in the tank circuit, but not to dispersion. Some of our early measurements were made with a one-quarter wave line. The operating frequency was moved from the resonance peak of the tank circuit, so that the detector was sensitive to both absorption and dispersion. Most of our measurements have been made with a length of $\frac{1}{8}$ wave, so that the detector was sensitive only to dispersion.

MEASURING METHOD

A. Longitudinal Relaxation Time, T_1

The longitudinal relaxation time, T_1 , has been determined as a function of temperature and magnetic field by observing the change of the magnetization of the He³ with time. For a given temperature and polarizing field, H , the magnetization of the He³ approaches its equilibrium value exponentially. The exponential growth or decay of the magnetization toward its equilibrium value at the field H was verified experimentally for three different initial states: (1) the sample was demagnetized by maintaining it in zero field for several T_1 's; (2) the sample was demagnetized at the field H_0 by rf saturation at the Larmor frequency; (3) the sample was negatively magnetized by an adiabatic fast passage.

The value of the magnetic field H during the relaxation process could be chosen between zero and 13.5 kilogauss. At precisely measured times during the relaxation process the magnetization was measured by means of a single adiabatic fast passage at the resonance field, H_0 , of 10 kgauss. The time necessary to change the field from H to H_0 was always less than 6 seconds. The peak amplitude of the resulting dispersion signal has been shown by Bloch⁸ to be proportional to the nuclear magnetization at the instant the passage through resonance is started. For fields near zero, the magnetization was allowed to decay from a high-field value.

⁸ F. Bloch, Phys. Rev. **70**, 460 (1946).

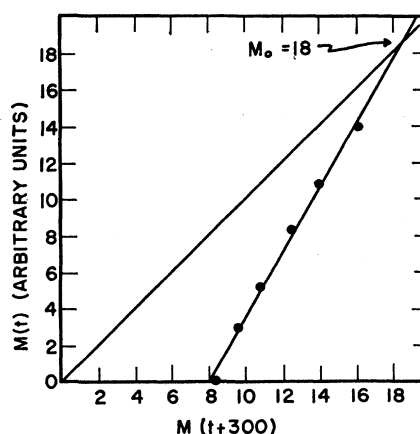


FIG. 3. Plot derived from the growth curve: $M(t)$ vs $M(t+300)$. The intersection point with the curve $M(t) = M(t+300)$ gives M_0 . T_1 can be determined from the slope.

If the sample is initially unmagnetized, then the growth curve is of the form $M(t) = M_0[1 - \exp(-t/T_1)]$, and both M_0 , the equilibrium value of the magnetization, and T_1 must be found from the experimental points. Values of M_0 and T_1 cannot be accurately obtained directly from a smooth curve drawn through the experimental points on an M versus t plot. Nevertheless, accurate values of M_0 and T_1 can be obtained from this smooth curve in a way suggested by Mangelsdorf.⁹ If we plot $M(t)$ versus $M(t+\tau)$ where τ is a constant of the order of T_1 , then we obtain the points shown in Fig. 3. Values of M_0 and T_1 can be determined from the best straight line through these points.

The error expected in a single measurement of a signal amplitude was only a few percent, resulting in $\pm 5\%$ deviations in the calculated values of T_1 . Larger variations in T_1 were attributed to periodic instrument instability.

B. Transverse Relaxation Time, T_2

The transverse relaxation time, T_2 , has been measured in a way which is not affected by magnetic field inhomogeneities or by atomic diffusion. In solids, the spin de-phasing interactions which determine the value of T_2 are strong, so that it is often possible to obtain T_2 from an observation of the linewidth of the absorption signal.⁵ It is considerably more difficult to resolve the absorption signal in liquids. The interactions leading to transverse relaxation are usually so small that spin de-phasing occurs because of the inhomogeneities in the large external z field, H_0 . The determination of T_2 in an inhomogeneous external field can be accomplished by Hahn's method of spin-echoes,¹⁰ which allows an extension of the range of measurable T_2 's by several orders of magnitude. However, the values of T_2 that can be measured by the spin-echo method are limited by

⁹ P. C. Mangelsdorf, Jr., J. Appl. Phys. **30**, 443 (1959).

¹⁰ E. L. Hahn, Phys. Rev. **80**, 580 (1950).

diffusion of the atoms in the inhomogeneous magnetic field. Other pulse techniques¹¹ have been developed to overcome the effects of field inhomogeneity and diffusion, and transverse relaxation times of several seconds have been observed.

Our method makes use of the integral solutions of the Bloch equations⁸ for large values of the rf field, H_1 . The rf field must be large enough to satisfy two conditions (the notation is that of Bloch):

1. The rf field must be very much larger than the inhomogeneities in the H_0 field over the sample. In most cases, this requires that $H_1 > 1$ gauss.
2. The integral solutions given by Bloch must be valid. This requires that $H_1 \gg 1/\gamma T_2$.

Under these conditions, two different techniques can be used to measure T_2 .

I. Direct Observation of the Transverse Decay¹²

The external field H_0 is held for several T_1 's at a value such that $\delta = (\gamma H_0 - \omega)/\gamma H_1 \gg (T_1/T_2)^{1/2}$. The magnetization grows to its equilibrium value M_0 . The value of δ is then reduced to zero in a time much shorter than T_1 or T_2 by varying the external field H_0 . The magnetization is thus rotated into the x - y plane and begins to precess at the Larmor frequency. H_1 is still applied so that the precession is driven by the rf field. If

$$\begin{aligned}\delta(t) &\gg (T_1/T_2)^{1/2} \quad \text{for } t < 0 \\ \delta(t) &= 0 \quad \text{for } t > 0\end{aligned}$$

then the solutions to the Bloch equations are:

$$\begin{aligned}M_{x,y} &= 0 \quad \text{for } t < 0 \\ M_y &= M_0 \sin(\omega t) \exp(-t/T_2) \quad \text{for } t > 0,\end{aligned}$$

where $\sin \omega t$ is replaced by $\cos \omega t$ to obtain M_x . The transverse magnetization therefore decays with a time constant T_2 . The induced voltage produced by this driven precession can be detected and then observed on a dc oscilloscope.

That the decay is unaffected by the inhomogeneities in H_0 can be seen by considering a simple model. Let us suppose that the sample is made up of a great many cells, in each of which the field is homogeneous. Let the field vary from cell to cell. The integral solutions to the Bloch equations will hold for each cell, and the driven magnetization vector in each cell will decay with the true spin-spin relaxation time. The value of δ will vary slightly from cell to cell, but if γH_1 is sufficiently large, δ will always be much smaller than one. The magnetization vectors of all the cells are forced to precess in

phase, according to the solutions given above, so that no de-phasing occurs due to the inhomogeneity in H_0 . A similar argument can be given to show that diffusion does not affect the decay. The diffusion of a magnetic moment from one cell to another only results in a small change in δ . The moment is still driven by the large rf field and precesses in phase with the other moments. If the rf field is not sufficiently large compared with the inhomogeneities in H_0 , then the decay time will be shorter than T_2 . The decay will be determined by the time required for a He^3 atom to diffuse through a distance over which the inhomogeneity in H_0 is comparable with H_1 . Some of our measurements of T_2 show this effect. If the value of H_1 is too small, T_2 is reduced. The T_2 values quoted below were taken at values of H_1 such that an increase or decrease of H_1 by a factor of two did not affect T_2 .

Redfield¹³ has shown that the transverse decay can be affected by the presence of a large driving field H_1 . In solids, a large value of H_1 can increase T_2 ,¹⁴ and if H_1 were increased further, Redfield's theory predicts that T_2 should approach T_1 . Redfield's arguments thus predict that the use of a large value of H_1 could lead to spuriously long values of T_2 in liquid He^3 . Since our values of T_2 are independent of H_1 when H_1 is changed by a factor of four, the size of H_1 does not seem to affect our T_2 measurements.

There is one effect that could lead to spuriously short values of T_2 . If radiation damping¹⁵ were present, the transverse decay would be affected by the reaction field produced by the detection coil. This field arises from the currents induced in the tuned circuit by the precessing magnetization. As pointed out by Bloembergen and Pound,¹⁶ radiation damping does not constitute a true relaxation mechanism. If relaxation effects are neglected, the magnetization \mathbf{M} satisfies the classical equation

$$\partial \mathbf{M} / \partial t = \gamma \mathbf{M} \times \mathbf{H},$$

where \mathbf{H} is the resultant field, including all reaction fields. Since $\partial \mathbf{M} / \partial t$ is perpendicular to \mathbf{M} , the magnitude of \mathbf{M} cannot change. Nevertheless, there are two ways in which the presence of a reaction field could produce an apparent reduction in T_2 .

(1) If the reaction field produced in the coil by the precessing magnetization is large enough to reduce the amplitude of H_1 significantly, then the transverse decay will be shortened due to the inhomogeneities in H_0 , as described above. This condition is certainly not satisfied in any of our experiments, since our detected signal is only a few millivolts, while the applied voltage is of the order of 2 volts.

¹¹ H. C. Torrey, Phys. Rev. **76**, 1059 (1949); R. Gabbillard, Phys. Rev. **85**, 694 (1952); H. Y. Carr and E. M. Purcell, Phys. Rev. **94**, 630 (1954); S. Meiboom and D. Gill, Rev. Sci. Instr. **29**, 688 (1958).

¹² This method has been developed and recently described by G. Bonera, L. Chiodi, L. Giulotto, and G. Lanzi, Nuovo cimento **14**, 119 (1959).

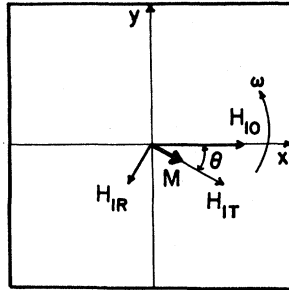
¹³ A. G. Redfield, Phys. Rev. **98**, 1787 (1955); see also B. V. Gokhale, Massachusetts Institute of Technology Quarterly Progress Report, MIT-55, October 15, 1959 (unpublished), p. 56.

¹⁴ N. Bloembergen and P. P. Sorokin, Phys. Rev. **110**, 865 (1958).

¹⁵ N. Bloembergen and R. V. Pound, Phys. Rev. **95**, 8 (1954).

(2) If the oscillation condition¹⁶ is satisfied, then the magnetization vector can proceed toward its equilibrium condition through radiating states. This would cause an increase in the rate of decay of the transverse component, and therefore a decrease in the apparent T_2 . We do not believe that our values of T_2 are shortened by this mechanism. It is true that the reaction field produced by the precessing magnetization can change the magnitude and direction of the resultant H_1 field, since the reaction field is in quadrature with \mathbf{M} (see Fig. 4). However, if adiabatic fast passage conditions are satisfied, the transverse magnetization will remain parallel to the resultant H_1 , \mathbf{H}_{1T} , as long as the reaction field, \mathbf{H}_{1R} , is smaller than the applied value of H_1 , \mathbf{H}_{10} . The magnetization will still be given by the above solutions to the Bloch equations, except that the magnetization will lag the applied field, \mathbf{H}_{10} , by a small angle θ . An absorption signal will be observed. The width of this signal would be due to radiation damping effects, as described by Bruce, Norberg, and Pake,¹⁷ but the transverse decay would not be affected. Maser action, due to the presence of the reaction field,

FIG. 4. Schematic diagram of the rf fields acting on the magnetization during an adiabatic fast passage when the magnetization is in the transverse plane. \mathbf{M} is the helium 3 magnetization; \mathbf{H}_{10} is the applied rf field; \mathbf{H}_{1R} is the reaction field induced by the precessing magnetization; \mathbf{H}_{1T} is the total rf field acting on the magnetization.



can therefore only occur when the reaction field is larger than the applied H_1 field.

Another argument against a shortening of T_2 by maser action is as follows. If this mechanism were effective in shortening T_2 , then an "exact signal"¹² should be observed when the H_0 field is swept away from resonance, since \mathbf{M} would not be reduced to zero. We have been unable to observe any residual signal under these conditions. In some cases, we have observed radiation effects and maser action following an adiabatic fast passage. A residual signal was observed in these cases, and the phenomena seem to be consistent with the theory proposed by Kemp.¹⁶ These effects will be described in the section on experimental results.

Figure 5 shows a transverse decay curve obtained in liquid He^3 at 1.2°K. T_2 has the value of 17 sec. Values of T_2 as long as 31 sec have been observed by this technique.

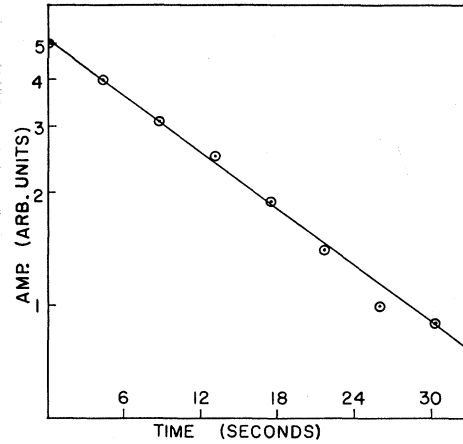


FIG. 5. Signal amplitude, in arbitrary units, as a function of time. This amplitude is proportional to the magnetization following the reduction of δ to zero, since the magnetization is precessing in the x - y plane.

II. Observation of the Steady-State Value of the Magnetization

In this modification, the steady state magnitude of the magnetization is determined as a function of δ . The field H_0 is held at some known value for several T_1 's. If the strength of the rf field H_1 is known (this can be calculated from the width of a fast passage signal), then δ will have a known value, Δ . After establishing equilibrium with some particular Δ , H_0 is swept quickly through the resonance condition. Thus, if

$$\delta(t) = \Delta \quad \text{for } t < 0$$

$$\delta(t) = \delta \quad \text{for } 0 < t \ll T_1 \text{ or } T_2$$

then the solutions to the Bloch equations are:

$$M_y = M_0 \sin(\omega t) \frac{\Delta}{\Delta^2 + T_1/T_2} \quad \text{for } t < 0$$

$$M_y = M_0 \sin(\omega t) \frac{\Delta}{\Delta^2 + T_1/T_2} \left(\frac{1 + \Delta^2}{1 + \delta^2} \right)^{\frac{1}{2}}$$

for $0 < t \ll T_1$ or T_2 .

The signal displayed on an oscilloscope as H_0 is swept through resonance looks very much like an ordinary adiabatic fast passage signal. The maximum amplitude, A , occurs when $\delta = 0$ and has the value

$$A = M_0 \frac{\Delta(1 + \Delta^2)^{\frac{1}{2}}}{\Delta^2 + T_0/T_2}.$$

This amplitude A is equal to the magnitude of the equilibrium magnetization for $\delta = \Delta$. Figure 6 shows the above function plotted for positive values of Δ and $T_1/T_2 = 21.6$. The circled points are the results obtained in liquid He^3 at 1.2°K. If T_1 and the rf field H_1 are known, T_2 can be calculated. For this case, $T_1 = 320$

¹⁶ James C. Kemp, J. Appl. Phys. **30**, 1451 (1959).

¹⁷ C. R. Bruce, R. E. Norberg, and G. E. Pake, Phys. Rev. **104**, 419 (1956).

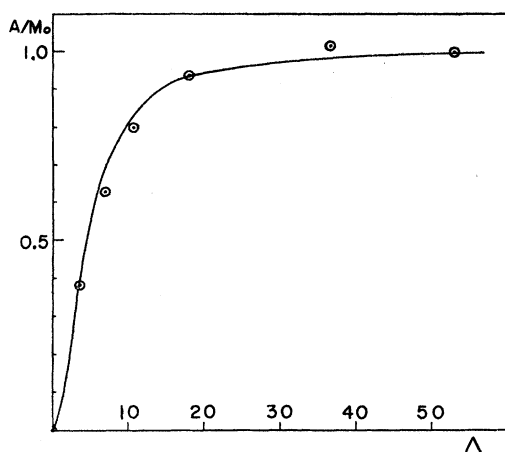


FIG. 6. The magnitude of the equilibrium magnetization for $\delta=\Delta$, in units of M_0 , as a function of Δ . The solid line is the equation given in the text. The points are the experimental observations.

sec, $H_1=3$ gauss, and $T_2=15$ sec. The two techniques give results that agree within the expected error.

Inhomogeneities in H_0 and diffusion do not affect the value of T_2 obtained in this way. The precession in the steady state at $\delta=\Delta$ is again driven by the large rf field, and small variations in δ from one part of the sample to another do not affect the amplitude given above. This method has some advantages when compared with the transverse decay method. To measure T_2 accurately with the transverse decay, the H_0 field must be swept quickly and accurately to $\delta=0$. This condition must be satisfied during the time of the decay. In the second method, δ must be held constant for several T_1 's, but the constancy is not as stringent as in the first method. Further, in the first method, the drift in the electronic equipment must be kept to a very

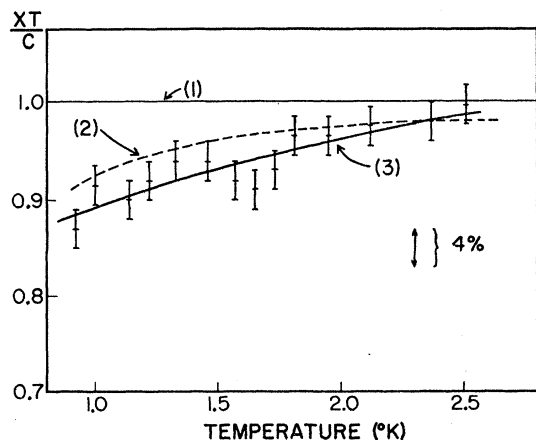


FIG. 7. Normalized susceptibility $\chi T/C$ as a function of temperature. (1) Curie-law curve. (2) Fermi gas curve for a degeneracy temperature of 0.45°K as obtained by Fairbank, Ard, and Walters.¹⁸ (3) Curve through data points of this research. Our points have been arbitrarily normalized to the Fermi curve at 2.0°K .

low level. This is not necessary with the second method. The second method does require an accurate determination of H_1 and a rather homogeneous H_1 .

EXPERIMENTAL RESULTS

The equilibrium value of the magnetization, M_0 , was measured as a function of magnetic field at a temperature of 2°K . The results show that M_0 is proportional to H as would be expected. These measurements are a check on our measuring technique at various fields. M_0 was also determined as a function of temperature at a field of 10 kgauss. The data of Fig. 7 show a deviation from Curie's Law which is in rough agreement with the work of Fairbank, Ard, and Walters.¹⁸ Our susceptibility data are normalized to the Fermi gas curve at 2.0°K , and seem to decrease more rapidly than the Fermi gas curve as the temperature is lowered. This indicates either that the degeneracy temperature is higher than the 0.45°K value reported by Fairbank, Ard, and

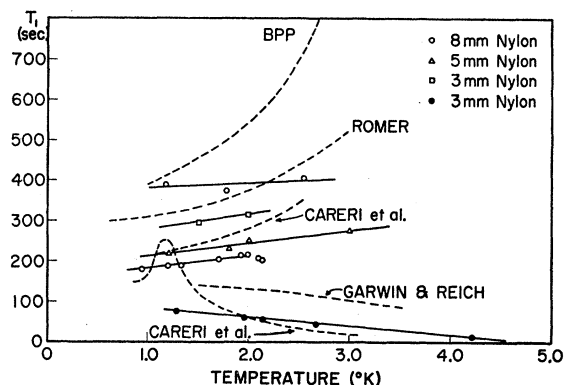


FIG. 8. Longitudinal relaxation time as a function of temperature, sample chamber size, and laboratory in which measurements were made. The BPP curve is formula (1) of the text.

Walters, or that the susceptibility approaches the Curie value above 1°K more gradually than predicted for an ideal Fermi gas. This question will be discussed at a later time when more accurate susceptibility data are available.

Figure 8 shows our results on the temperature dependence of T_1 . The points are relaxation times measured in various nylon containers at 10 kgauss. The dashed curves show the relaxation times obtained by other workers at various magnetic fields (these fields are indicated in Fig. 9). Some measurements of T_1 were made in nylon chambers lined with carefully cleaned pyrex and with waxed paper. These results are reported in Table I. A time effect was observed in some series of runs in which the sample chamber was not opened. T_1 was found to increase monotonically with run number as long as air was not admitted to the sample chamber. In some runs, we observed a decrease

¹⁸ W. M. Fairbank, W. B. Ard, and G. K. Walters, Phys. Rev. 95, 566 (1954).

of T_1 with time following the condensation of the He³. In these runs, the sample chamber filling the tube had a $\frac{1}{8}$ -in. i.d., and it is possible that oxygen was diffusing into the liquid He³.

Figure 9 shows our results on the field dependence of T_1 at 2°K measured in a 3-mm nylon chamber. The minimum field was about 1 gauss. A qualitatively similar behavior was found in other chambers at other temperatures with different T_1 values, but the field dependence was not thoroughly investigated in these chambers. The dips at 10.5 kgauss and 5.3 kgauss were reproducible within the experimental error. Some of the scatter in our results is due to the time effects previously mentioned. In a single run, T_1 values with a scatter of approximately $\pm 5\%$ are obtained. The data of Garwin and Reich at 1.7 kgauss fall close to our curve. Romer's measurements of T_1 at 6 different fields are also shown in Fig. 9.

Our measured values of T_2 are given in Table I. Most of the values were obtained by direct observation

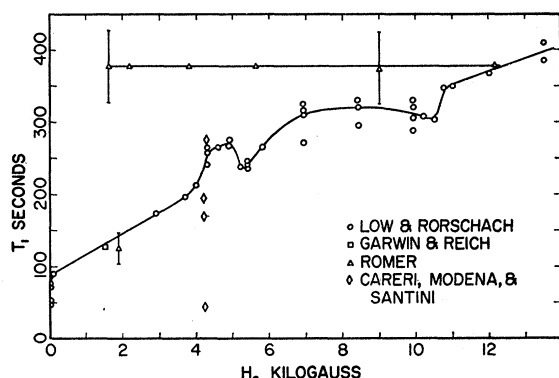


FIG. 9. The longitudinal relaxation time T_1 as a function of applied magnetic field H in a 3-mm nylon sample chamber at 2.0°K. The results of other workers are also shown.

of the transverse decay. Some of the values were checked by observation of the steady-state value of the magnetization. The two methods always agreed within the experimental error. At temperatures near 1.9°K, T_2 appears to be close to 30 sec, independent of sample chamber size. At temperatures near 1.2°K, it is possible that T_2 is somewhat less. There is some variation in T_2 from one sample chamber to another at 1.2°K.

Some of our measurements at the lowest temperatures exhibited radiation bursts following the adiabatic fast passage signal (Fig. 10). A preliminary report of these measurements has already been published.¹⁹ We attribute these bursts to nuclear maser operation in He³. Somewhat different observations of radiation damping and nuclear maser operation in benzene have been recently reported by Szöke and Meiboom.²⁰ Our measurements show several radiation bursts similar to

TABLE I. Values of T_1 and T_2 as a function of temperature in various sample chambers.

Chamber	Temp (°K)	T_1 (sec)	T_2 (± 5 sec)
3-mm nylon No. 1	1.2	320	20
	1.5		30
	2.0	370	30
3-mm glass No. 1 8-mm nylon	1.2	75	20
	1.9	200	25
	1.2	200	30
3-mm nylon No. 2	1.3	100	10
3-mm nylon No. 3	1.8	150	30
4-mm wax paper	1.2	220	30
3-mm glass No. 2	2.0	155	
	1.2	175	

those observed in electron resonance by Feher *et al.*²¹ and Chester *et al.*²² We believe these radiation bursts are due to energy exchange between the nuclear system and the tuned circuit as described by Bloembergen and Pound,¹⁵ and more recently by Kemp.¹⁶ These observations were made with a one-quarter wavelength transmission line and with the operating frequency adjusted so that the detector was sensitive both to absorption and dispersion.

The three bursts of radiation shown in Fig. 10 were observed at the lowest temperatures when the magnetization exceeded a critical value. For this sample chamber, $T_1=320$ sec and $T_2=30$ sec. The temperature was 1.3°K, $H_0=10$ kgauss and $H_1=3$ gauss. The bursts have a repetition frequency of about 50 cps, and the envelope of the decay has a time constant of about 20 milliseconds. The signal amplitude is 20 mv. For a given value of H_1 and dH_0/dt , there is a critical magnetization below which the radiation does not occur. Smaller values of H_1 and dH_0/dt favor a smaller critical magnetization. An adiabatic fast passage immediately following the radiation bursts shows that M_z is diminished but still inverted.

Most of the above observations can be explained in a qualitative way with the results of Kemp.¹⁶ The oscillation condition for spontaneous emission can be written as $\tau_R < T_2^*$, where $\tau_R = 1/\gamma M_0 Q$ and $T_2^* = 1/\gamma \Delta H$. M_0 is the magnetization per unit volume of the sample at temperature T , Q is the coil quality factor, γ the gyromagnetic ratio, and ΔH the resonance line width. For the above observations $\tau_R \approx 1/600$ sec and $T_2^* \approx 1/400$ sec for $T=1^\circ\text{K}$, $H_0=10$ kgauss and

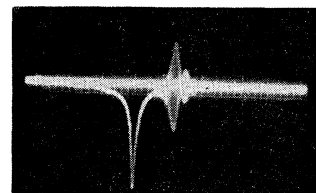


FIG. 10. Radiation burst following an adiabatic fast passage (see text).

¹⁹ H. E. Rorschach, Jr., and F. J. Low, *Quantum Electronics* (Columbia University Press, New York, 1960), p. 177.

²⁰ A. Szöke and S. Meiboom, *Phys. Rev.* **113**, 585 (1959).

²¹ G. Feher, J. P. Gordon, E. Buehler, E. A. Gere, and C. D. Thurmond, *Phys. Rev.* **109**, 221 (1958).

²² P. F. Chester, P. E. Wagner, and J. G. Castle, Jr., *Phys. Rev.* **110**, 281 (1958).

$\Delta H = 0.02$ gauss. It is therefore reasonable to suppose that the oscillation condition is responsible for the observed critical value of the magnetization, and that cumulative dephasing reduces the magnetization during the radiation process so that the oscillation condition is no longer satisfied. The magnetization would not return to equilibrium, but could be left inverted, as described by Kemp. We are unable to account quantitatively for the repetition rate of the bursts, or for the dependence of the critical magnetization on H_1 or dH_0/dt .

CONCLUSIONS

A. Longitudinal Relaxation Time

The Bloembergen, Purcell, and Pound theory for relaxation in ordinary fluids⁵ has been applied to liquid He^3 by other workers.¹⁻⁴ Since the diffusion coefficient, D , of liquid He^3 has been measured,³ the correlation time τ_c can be estimated²³: $\tau_c \approx \langle r^2 \rangle / 12D = 10^{-12}$ sec, where $\langle r^2 \rangle$ is the mean-square interatomic distance. Since $\tau_c \ll 1/\omega_0$ for any reasonable magnetic field, the longitudinal relaxation time is given approximately by²³

$$\left(\frac{1}{T_1} \right)_{\text{He}} \approx \frac{2\pi \gamma^4 \hbar^2 N_0}{5 a D}, \quad (1)$$

where N_0 is the concentration of He^3 atoms, a is the distance of closest approach and γ is the gyromagnetic ratio. This function is plotted in Fig. 10, with $a = 2.5\text{\AA}$. Further, the transverse relaxation time T_2 should be equal to T_1 , and both should be independent of magnetic field. The temperature and pressure dependence of T_1 is due to the dependence of N_0 and D on these quantities.

The results presented in the previous section clearly indicate that impurity relaxation is present. Two kinds of impurity relaxation may play a role.

1. Wall relaxation. The wall surfaces of the sample chamber may be paramagnetic, or contaminated with adsorbed paramagnetic impurities (such as oxygen). If all nuclei relax immediately when they strike a wall, then the relaxation time will depend only on the diffusion coefficient D and the diameter d of the cylindrical sample chamber. A dimensional analysis suggests that $(1/T_1)_{\text{wall}} \approx D/d^2 = 1/100 \text{ sec}^{-1}$, for $d = 1 \text{ mm}$ and $D = 10^4 \text{ cm}^2/\text{sec}$. The apparent relaxation time is thus inversely proportional to D .

2. Bulk impurity relaxation. The liquid He^3 may contain paramagnetic impurities in suspension. A bulk impurity relaxation similar to that caused by paramagnetic ions in solution in ordinary liquids may then occur. This case has been treated by Bloembergen, Purcell, and Pound, and we will assume their expression valid for impurities in He^3 :

$$\left(\frac{1}{T_1} \right)_{\text{imp}} \approx \left(\frac{1}{T_1} \right)_{\text{He}} \left(\frac{\mu_{\text{imp}}^2}{\mu_{\text{He}}^2} \right) \left(\frac{N_{\text{imp}}}{N_0} \right),$$

²³ H. C. Torrey, Suppl. Nuovo cimento **9**, 95 (1958).

where N_{imp} = the concentration of impurities with magnetic moment μ_{imp} . Thus, both the bulk impurity and the intrinsic relaxation times in He^3 should be directly proportional to the diffusion coefficient if the Bloembergen, Purcell, and Pound theory is applicable. Since the magnetic moment of a paramagnetic impurity is approximately 1000 times the moment of a He^3 nucleus, an impurity concentration of about one part in 10^6 is all that is required to produce an impurity relaxation comparable with that expected in the bulk liquid. The above expression for $(1/T_1)_{\text{imp}}$ is valid if the diffusion coefficient for the impurity is equal to that of the He^3 . If the impurity diffusion coefficient is considerably smaller than that of He^3 , then bulk impurities could lead to a relaxation time having the same dependence on D as wall relaxation.

The data of Fig. 8 indicate that there is no regular dependence of T_1 on sample chamber size. This seems to indicate either that a bulk relaxation is operative, or that any wall relaxation is due to adsorbed impurities, such as oxygen, rather than to intrinsically paramagnetic walls. With the exception of one set of data of Careri *et al.*,¹ the shorter relaxation times increase as the temperature is lowered, and the longer relaxation times decrease as the temperature is lowered.

We can understand the above mentioned temperature dependence and also the pressure dependence reported by Garwin and Reich³ if we assume that the net inverse relaxation time is a sum of two parts:

$$\begin{aligned} (1/T_1)_{\text{net}} &= (1/T_1)_{\text{wall}} + (1/T_1)_{\text{bulk}} \\ &= C_1 D + C_2 \rho / D \end{aligned}$$

D is the diffusion coefficient and ρ the density of the liquid. (We also assume that the density of any bulk impurities is proportional to the liquid density.) This

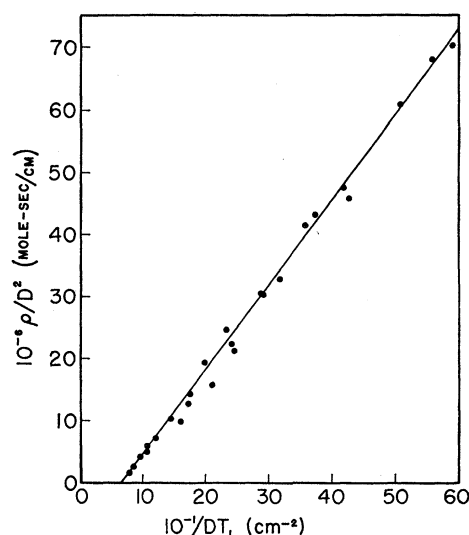


FIG. 11. $1/DT_1$ vs ρ/D^2 . The points are obtained from measurements of D and T_1 as a function of pressure and temperature reported by Garwin and Reich.³

assumption can be tested by plotting $1/DT_1$ vs ρ/D^2 (the diffusion coefficient D and T_1 vary with pressure and temperature). Our assumption predicts a linear relation. Figure 11 shows this plot for the data reported by Garwin and Reich. Points have been taken from their curves at temperatures between 1.5 and 3.0°K and at pressures from 2.38 to 67.0 atm. The density values are those reported by Sherman and Edeskuty.²⁴ The bulk relaxation is determined by the slope and the wall relaxation by the intercept. Extrapolating to the vapour pressure at 2.0°K, we find $(T_1)_{\text{wall}}=200$ sec and $(T_1)_{\text{bulk}}=400$ sec. This bulk value is in good agreement with Romer's results. If we plot Romer's results in the same way, we find $(T_1)_{\text{wall}}=2000$ sec and $(T_1)_{\text{bulk}}=400$ sec at 2.0°K. The good agreement of the values for $(T_1)_{\text{bulk}}$ suggests that these values represent the true values for the pure liquid. If any bulk impurities are present, their diffusion coefficient must be small enough to produce relaxation having the same dependence on D as the wall relaxation.

The field dependence shown in Fig. 9 indicates the presence of impurities, since a field-dependent T_1 does not seem to be a property of the pure bulk liquid.² The dependence of T_1 on field is probably due to a strongly field-dependent wall relaxation. If, however, paramagnetic impurities were present in the bulk liquid, the observed dependence of T_1 on field could be due to the interaction of the impurity spin with the excitations in the liquid.

The Bloembergen, Purcell, and Pound theory seems adequate to explain the T_1 data above 1°K, if a contribution from impurity relaxation of the form $1/T_1 \propto D$ is assumed. Romer's results thus seem to represent true bulk relaxation times, except at the highest temperatures. The results of Romer and of Garwin and Reich are both consistent with (1) if a , the distance of closest approach, is taken as 1.6Å. It thus appears that wall effects can be compensated and true bulk relaxation times determined if T_1 is measured as a function of pressure or temperature.

B. Transverse Relaxation Time

We have obtained values for T_2 at a field of 10 kgauss of the order of 30 seconds independent of the size of the sample chamber or the value of T_1 . If wall interactions were entirely responsible for the transverse relaxation, then the value of T_2 in the various chambers

would be governed by diffusion to the walls and by the strength of the wall interaction. T_2 will have its smallest value when the wall interaction is strong (immediate relaxation at the wall); the value of T_2 will then be determined by the diffusion coefficient and the size of the sample chamber. The solution of the diffusion equation for cylindrical symmetry²⁵ leads to a relaxation time $T_2 \approx r^2/6D$, where r is the radius of the chamber. For the 3-mm chamber, $r^2/6D \approx 35$ seconds, which is consistent with the observed values of T_2 . For the 8-mm chamber, however, $r^2/6D \approx 245$ seconds, and it is impossible to explain the values of T_2 by wall relaxation. We therefore conclude that wall effects are not important in determining the value of T_2 .

If the value of T_2 is determined by the dipolar interaction in the pure liquid, then the Bloembergen, Purcell, and Pound theory can be used to estimate the size of T_2 . This theory predicts that $T_1 = T_2$ for a pure liquid if $\tau_c \ll 1/\omega_0$. Since $\tau_c \approx 10^{-12}$ sec for liquid helium 3, the equality of T_1 and T_2 in the pure liquid should hold for all magnetic fields less than $H \approx 1/\gamma\tau_c \approx 10^8$ gauss. Thus our values of T_2 are too short to agree with the Bloembergen, Purcell, and Pound theory. Redfield's arguments do not remove this inconsistency. His modified Bloch equations predict that the presence of the large rf field H_1 can only lengthen T_2 , so that the true T_2 must be even shorter than 30 seconds.

The low value of T_2 may be due to the presence of some bulk paramagnetic impurity. If the spin-lattice relaxation time of the impurity spin were sufficiently long, so that the correlation time becomes comparable to the Larmor period, then T_2 would be appreciably smaller than T_1 .⁵ Bloembergen²⁶ has also suggested an impurity spin-exchange interaction with a correlation time sufficiently long to produce $T_2 \ll T_1$. This mechanism is operative in some aqueous solutions and may be operative in liquid helium 3, leading to the small values of T_2 and the field dependence of T_1 .

ACKNOWLEDGMENTS

The authors are indebted to Dr. Careri, Dr. Fairbank, Dr. Garwin, Dr. Reich, Dr. Romer, and Dr. Walters for helpful comments and preprints of their work. We would also like to thank Mr. Belcher, Mr. Surles, and Mr. Vander Henst for technical assistance.

²⁴ R. H. Sherman and F. J. Edeskuty, *Ann. Phys.*, **9**, 522 (1960).

²⁵ Arnold Sommerfeld, *Partial Differential Equations in Physics* (Academic Press, Inc., New York, 1949), p. 102.

²⁶ N. Bloembergen, *J. Chem. Phys.*, **27**, 572 (1957).

FIG. 10. Radiation burst
following an adiabatic fast
passage (see text).

